

Long-lived states of oscillator chain with dynamical traps

Ihor Lubashevsky¹, Reinhard Mahnke², Morteza Hajimahmoodzadeh³, and Albert Katsnelson³

¹ General Physics Institute named after A.M. Prohorov, Russian Academy of Sciences, Vavilov str., 38, 119991 Moscow, Russia, e-mail: ialub@fpl.gpi.ru

² Fachbereich Physik, Universität Rostock, D 18051 Rostock, Germany, e-mail: reinhard.mahnke@physik.uni-rostock.de

³ Faculty of Physics, M.V. Lomonosov Moscow State University, Moscow 119992, Russia, e-mail: albert@solst.phys.msu.su

Received: date / Revised version: date

Abstract. A simple model of oscillator chain with dynamical traps and additive white noise is considered. Its dynamics was studied numerically. As demonstrated, when the trap effect is pronounced nonequilibrium phase transitions of a new type arise. Locally they manifest themselves via distortion of the particle arrangement symmetry. Depending on the system parameters the particle arrangement is characterized by the corresponding distributions taking either a bimodal form, or twoscale one, or unimodal onescale form which, however, deviates substantially from the Gaussian distribution. The individual particle velocities exhibit also a number of anomalies, in particular, their distribution can be extremely wide or take a quasi-cusp form. A large number of different cooperative structures and superstructures made of these formations are found in the visualized time patterns. Their evolution is, in some sense, independent of the individual particle dynamics, enabling us to regard them as dynamical phases.

PACS. 05.40.-a Fluctuation phenomena, random processes, noise, and Brownian motion – 05.45.-a Non-linear dynamics and nonlinear dynamical systems – 05.70.Fh Phase transitions: general studies

1 Introduction

For the last several decades various phenomena cause by the ordering action of noise in nonequilibrium systems are found (for a general review see Refs. [1, 2, 3, 4]). Popular examples are stochastic resonance [5, 6, 7], coherence resonance [2, 8], noise-induced transport [9], and noise-induced phase transitions [3, 10, 11]. Typically the latter are due to multiplicative noise. However, additive noise in the presence of other multiplicative noise can also induce phase transitions [12, 13, 14] or individually cause a hidden phase transition to become visible [15].

The constructive role of noise is peculiar to nonequilibrium systems only. In thermodynamic systems, for example, the phase formation is solely due to a certain regular “force” changing its form, in particular, the number of stationary points. Available noise mainly perturbs the system motion around these points.

In the present paper we pay attention to a new class of nonequilibrium systems, namely, many particle ensembles where some long-lived cooperative states can form whereas the regular component of “individual” forces has no stationary points except for one corresponding to the homogeneous state. The latter, in addition, is locally stable for all the values of the system parameters. Besides, only additive noise enters such systems.

Originally investigation of the model under consideration was stimulated by a wide class of intricate cooperative phenomena found in the dynamics of vehicle ensembles moving on highways, motion of fish and bird swarms, stock markets, *etc* (for a review see Ref. [16]). The model background is the following. People as elements of a certain system cannot individually control all the governing parameters. Therefore one chooses a few crucial parameters and focuses on them the main attention. When the equilibrium with respect to these crucial parameters is attained the human activity slows down retarding, in turn, the system dynamics as a whole. For example, in driving a car the control over the relative velocity is of prime importance in comparison with the correction of the headway distance. So under normal conditions a driver, first, should eliminate the relative velocity between his car and a car ahead and only then optimize the headway.

These speculations have led us to the concept of dynamical traps, a certain “low” dimensional region in the phase space where the main kinetic coefficients specifying the time scales of the system dynamics become sufficiently large in comparison with their values outside the trap region [17, 18, 19, 20]. As a result long-lived states have to appear. In time patterns these states manifest themselves like a sequence of fragments within which at least one of the phase variables remains approximately

constant. These fragments are continuously connected by sharp jumps of the given variable. Paper [18] demonstrated that such long-lived states do exist in the dense traffic flow and proposed some model of dynamical traps to explain the observed features of car velocity time series. Papers [19,20] simplified this model to single out the dynamical trap effect in its own record. Similar phenomena seem to be observed in physical systems also, for example, during the non-monotonic relaxation of Pd-metal alloys charged with hydrogen [21]. Paper [19] studied a single oscillator with dynamical traps and demonstrated numerically that white noise can cause the distribution function of oscillator position to convert from the unimodal form to the bimodal one. It is due to the fact that inside the trap region the regular “force” is depressed only rather than changes the sign and the system motion is mainly caused by a random Langevin “force”. A first step towards of this effect in oscillator ensembles was made in Ref. [20]. In particular, the dynamical traps were demonstrated to be able to give rise to the system instability and an anomalous velocity distribution like a cusp $\propto \exp\{-|v|\}$ smoothed, naturally, inside a narrow transition region. It should be noted that similar anomalous velocity distributions were found for dense traffic flow [22].

The purpose of the present paper is to demonstrate that an ensemble of such oscillators with dynamical traps can exhibit a number of anomalous cooperative phenomena, their detailed investigation will be published elsewhere. However, first, we clarify the relation between the specific mathematical form of the model to be studied and the concept of dynamical traps discussed above.

Motivated behavior of particles

Keeping in mind the aforesaid about the human behavior we consider a one-dimensional ensemble of “lazy” particles characterized by their positions and velocities $\{x_i, v_i\}$ as well as possessing some motives for active behavior. Particle i wants to get the “optimal” middle position between the nearest neighbors. So one of the stimuli for it to accelerate or decelerate is the difference $\eta_i = x_i - \frac{1}{2}(x_{i-1} + x_{i+1})$ provided its relative velocity $\vartheta_i = v_i - \frac{1}{2}(v_{i-1} + v_{i+1})$ with respect to the pair of the nearest neighbors is sufficiently low. Otherwise, especially if particle i is currently located near the optimal position, it has to eliminate the relative velocity, being the other stimulus for particle i to change its state of motion. Since a particle cannot predict the dynamics of its neighbors it has to regard them as moving uniformly with the current velocities. So both the stimuli are to determine directly its acceleration dv_i/dt . The model to be formulated in the next section combines both of these stimuli within a linear approximation similar to $(\eta_i + \sigma\vartheta_i)$, where σ is the relative weight of the second stimulus.

When, however, the relative velocity ϑ_i of particle i attains sufficiently low values the current situation for it cannot become worse, at least, rather fast. So in this case particle i prefers not to change the state of motion and to

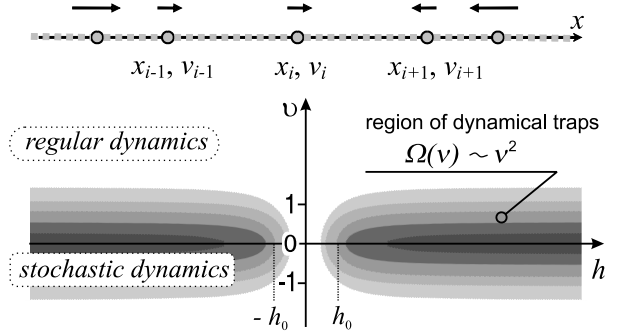


Fig. 1. The particle ensemble under consideration and the structure of the phase space. The darkened region depicts the points where the dynamical trap effect is pronounced. For the relationship between the variables x_i , v_i , h_i , and ϑ_i see formulae (4) and (5).

retard the correction of its relative position. This assumption leads to the appearance of some common cofactor $\Omega(\vartheta_i)$ in the governing equation like this

$$\frac{dv_i}{dt} \propto -\Omega(\vartheta_i)(\eta_i + \sigma\vartheta_i).$$

The cofactor $\Omega(\vartheta)$ is to meet the inequality $\Omega(\vartheta) \ll 1$ for $\vartheta \ll \vartheta_c$ and $\Omega(\vartheta) \approx 1$ when $\vartheta \gg \vartheta_c$, where ϑ_c is a certain critical value quantifying the particle perception of speed. Exactly the appearance of such a factor is the implementation of the dynamical trap effect. Now let us specify the model.

2 Model

The following linear chain of N point-like particles is considered (Fig. 1). Each internal particle $i \neq 1, N$ can freely move along the x -axis interacting with the nearest neighbors, namely, particles $i - 1$ and $i + 1$ via ideal elastic springs with some quasi-viscous friction. The dynamics of this particle ensemble is governed by the collection of coupled equations

$$\frac{dx_i}{dt} = v_i, \quad (1)$$

$$\frac{dv_i}{dt} = -\Omega(\vartheta_i, h_i)[\eta_i + \sigma\vartheta_i + \sigma_0 v_i] + \epsilon\xi_i(t). \quad (2)$$

Here for $i = 2, 3, \dots, N - 1$ the variables η_i and ϑ_i to be called the symmetry distortion and the distortion rate, respectively, are specified as

$$\eta_i = x_i - \frac{1}{2}(x_{i-1} + x_{i+1}), \quad (3)$$

$$\vartheta_i = v_i - \frac{1}{2}(v_{i-1} + v_{i+1}), \quad (4)$$

the mean distance h_i between the particles at the point x_i , by definition, is

$$h_i = \frac{1}{2}(x_{i+1} - x_{i-1}), \quad (5)$$

and $\{\xi_i(t)\}$ is the collection of mutually independent white noise sources of unit amplitude, i.e.

$$\langle \xi_i(t) \rangle = 0, \quad \langle \xi_i(t) \xi_{i'}(t') \rangle = \delta_{ii'} \delta(t - t'). \quad (6)$$

In addition, the parameter ϵ is the noise amplitude, σ is the viscous friction coefficient of the springs, σ_0 is a small parameter that can be treated as a certain viscous friction related to the particle motion with respect to the given physical frame. It is introduced to prevent the system motion as a whole with infinitely high velocity. Besides, the symbol $\langle \dots \rangle$ denotes averaging over all the noise realizations, $\delta_{ii'}$ and $\delta(t - t')$ are the Kronecker symbol and the Dirac δ -function. The factor $\Omega(\vartheta, h_i)$ is due to the effect of dynamical traps and actually following our previous paper [17] the *Ansatz*

$$\Omega(\vartheta, h) = \frac{\vartheta^2 + \Delta^2(h)}{\vartheta^2 + 1} \quad (7)$$

with a function $\Delta(h)$ such that

$$\Delta^2(h) = \Delta^2 + (1 - \Delta^2) \frac{h_0^2}{h^2 + h_0^2} \quad (8)$$

is used. The parameter $\Delta \in [0, 1]$ quantifies the dynamical trap influence and the spatial scale h_0 specifies the small distances within which the trap effect is to be depressed, i.e. for $h \ll h_0$ the value $\Delta(h) \approx 1$ whereas when $h \gg h_0/\Delta$ the value $\Delta(h) \approx \Delta$. If the parameter $\Delta = 1$, the dynamical traps do not exist at all, in the opposite case, $\Delta \ll 1$, their influence is pronounced inside a certain neighborhood of the h -axis (trap region) whose thickness is about unity (Fig. 1). The temporal and spatial scales have been chosen so that the thickness of the trap region be about unity as well as the oscillation circular frequency be also equal to unity outside the trap region. The terminal particles, $i = 1$ and $i = N$, are assumed to be fixed, i.e.

$$x_1(t) = 0, \quad x_N(t) = (N - 1)l, \quad (9)$$

where l is the particle spacing in the homogeneous chain. The particles are treated as mutually impermeable ones. So when the coordinate x_i and x_{i+1} of an internal particle pair become identical the absolutely elastic collision is assumed to happen, i.e. if $x_i(t) = x_{i+1}(t)$ at a certain time t then the timeless velocity exchange

$$\begin{aligned} v_i(t+0) &= v_{i+1}(t-0), \\ v_{i+1}(t+0) &= v_i(t-0) \end{aligned} \quad (10)$$

comes into being. The multiparticle collisions are ignored.

The system of equations (1)–(10) forms the model under consideration.

The stationary point $x_i^{\text{st}} = (i - 1)l$ is stable with respect to small perturbations. It stems from the linear stability analysis with respect to perturbations of the form

$$\delta x_i(t) \propto \exp\{\gamma t + \mathbf{i}kl(i - 1)\}, \quad (11)$$

where γ is the instability increment, k is the wave number, and the symbol \mathbf{i} denotes the imaginary unite. The

boundary conditions (9) are fulfilled by assuming the wave number k to take the values $k_m = \pi m / [(N - 1)l]$ for $m = \pm 1, \pm 2, \dots, \pm(N - 2)$. For large values of the particle number N the parameter k can be treated as a continuous variable. Using the standard technique the system of equations (1), (2) for perturbation (11) leads us to the following relation of the instability increment $\gamma(k)$ and the wave number k :

$$\begin{aligned} \gamma &= -\Omega_0 \left[\frac{1}{2} \sigma_0 + \sigma \sin^2 \left(\frac{kl}{2} \right) \right] \\ &+ \mathbf{i} \sqrt{2\Omega_0 \sin^2 \left(\frac{kl}{2} \right) - \Omega_0^2 \left[\frac{1}{2} \sigma_0 + \sigma \sin^2 \left(\frac{kl}{2} \right) \right]^2}. \end{aligned} \quad (12)$$

In deriving expression (12) *Ansatz* (7) has been used, enabling us to set $\Omega_0 = \Omega(0, l) = \Delta^2(l)$. Whence it follows that $\text{Re } \gamma(k) > 0$ for $k > 0$, so the homogeneous state of the chain is stable with respect to infinitely small perturbations of the particle arrangement.

3 Nonlinear dynamics

The nonlinear dynamics of the given system has been analyzed numerically. The integration of the stochastic differential equations (1), (2) was performed using the E2 high order stochastic Runge-Kutta method [23] (see also work [24]). Particle collisions were implemented analyzing a linear approximation of the system dynamics within *one* elementary step of the numerical procedure and finding the time at which a collision has happened. Then this step treated as a complex one was repeated. The integration time step of 0.02 was used, the obtained results had been checked to be actually stable with respect to decreasing the integration time step. The ensemble of 1000 particles was studied in order to make the statistics sufficient and to avoid a strong effect of the boundary conditions. The integration time T was chosen from 5000 to 8000 time units in order to make calculated distributions stable. At the initial stage all the particle were distributed uniformly in space whereas their velocities were randomly and uniformly distributed within the unit interval.

The results of numerical simulation were used to evaluate the following partial distributions

$$\mathcal{P}(z) = \frac{1}{(N - 2M)(T - T_0)} \sum_{i=M}^{N-M} \int_{T_0}^T dt \delta(z - z_i(t)), \quad (13)$$

where the time dependence $z_i(t)$ describes the dynamics of one of the variables $\eta_i(t)$, $\vartheta_i(t)$, and $v_i(t)$ ascribed to particle i and z is a given point of the space \mathbb{R}_z describing the symmetry distortion η , the distortion rate ϑ , and the particle velocity v , respectively. The variables $\{\eta, \vartheta, v\}$ enable one to represent the system dynamics portrait within the space $\mathbb{R}_\eta \times \mathbb{R}_\vartheta \times \mathbb{R}_v$ or its subspace. Besides, N is the total number of particles in the ensemble and M is the number of particles located near each of its boundaries. They

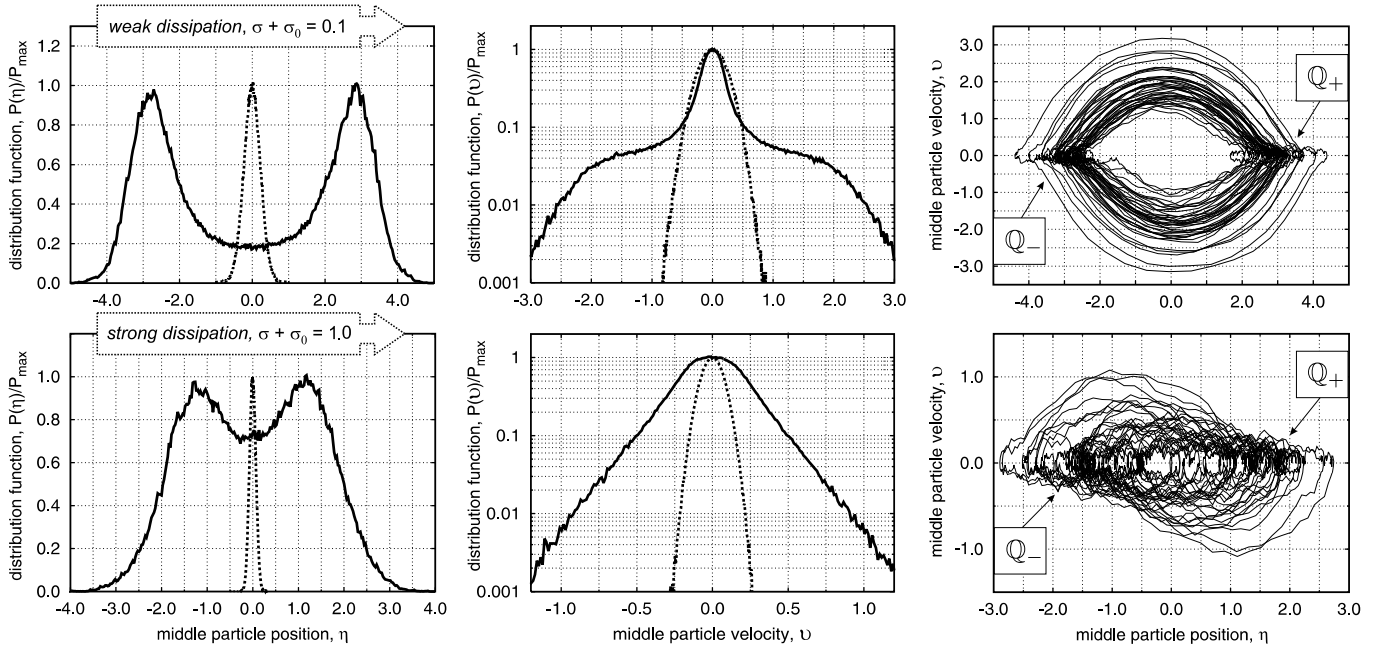


Fig. 2. The distribution functions of the coordinate η and the velocity ϑ of the movable particle in the 3-particle ensemble. These distributions were obtained by averaging the simulation results over time interval of 100000. Solid lines correspond to the case of strong trap effect, $\Delta = 0.1$, dotted line match the absence of dynamical traps, $\Delta = 1.0$. The right widows depict some path fragment formed by the movable particle during time interval of 1000 time units. Other used parameters are $\epsilon = 0.1$ and two values of the dissipation rate $\sigma + \sigma_0 = 0.1$ (upper row) and $\sigma + \sigma_0 = 1.0$ (lower row).

are excluded from the consideration in order to weaken a possible effect of the specific boundary conditions. The same concerns the lower boundary of time integration T_0 , its value is chosen to eliminate the effect of the specific initial conditions.

The numerical implementation of the integration over time in expression (13) was related to the direct summation of the obtained time series and the partition of the corresponding space \mathbb{R}_z was chosen so that the results be practically independent of the cell size. The value of M was also chosen using the result stability with respect to the double increase in M . Typically the value $M \sim 50$ was chosen for $N = 1000$, for $N = 3$, naturally, $M = 1$, and $T_0 \sim 500-1000$.

3.1 Three particle ensemble

The given oscillator chain made of three particles is actually the system studied in part previously [17]. In this case only the middle particle is movable and the variables $\eta := \eta_2$ and $\vartheta := \vartheta_2$ are its coordinate and velocity. Here we also present the results for the 3-particle ensemble in order to have a feasibility of distinguishing characteristics of local nature from many particle effects.

Figure 2 compares the distribution functions $\mathcal{P}(\eta)$ and $\mathcal{P}(\vartheta)$ obtained in the cases where the dynamical trap effect is absent ($\Delta = 1$) and when the dynamical traps affect the particle motion substantially ($\Delta \ll 1$). The upper windows correspond to the system with weak dissipation,

$\sigma + \sigma_0 = 0.1$, whereas the lower ones are related to the case of strong dissipation, $\sigma + \sigma_0 = 1.0$

In agreement with the previous results [17] it is seen that the decrease of the parameter Δ , i.e. the dynamical trap intensification induces the conversion of the function $\mathcal{P}(\eta)$ from the unimodal form to the bimodal one, with the dissipation no more then weakening this effect. A new result is the essential dependence of the velocity distribution on the dissipation rate. In the case of weak dissipation the movable particle performs alternatively fast motions outside the trap region and slow motion inside it. The fast motion paths connect the neighborhoods Q_- , Q_+ of the $\mathcal{P}(\eta)$ -function maxima, whereas the slow motion arises when the particle wanders inside these regions. This feature is visualized in Fig. 2, the right upper window shows a fragment of the particle path of duration about 1000 time units. Therefore the obtained distribution function $\mathcal{P}(\vartheta)$ as seen in Fig. 2 (middle upper window) actually is made of two monoscale components. For the case of strong dissipation the two neighborhoods Q_- and Q_+ are not directly connected by the fast motion paths (Fig. 2, right lower window). Now they rather uniformly spread over a certain domain on the $\{\eta, \vartheta\}$ -plane, previously, they were located inside a sufficiently narrow layer. As a result the velocity distribution converts into a monoscale function having a quasi-cusp form $\propto \exp\{-|\vartheta|\}$. We relate the cusp formation to the properties of the system dynamics near the trap region. It is justified in Fig. 3 showing the resulting velocity distribution of the movable particle when noise and dissipation are absent. In this case the 3-

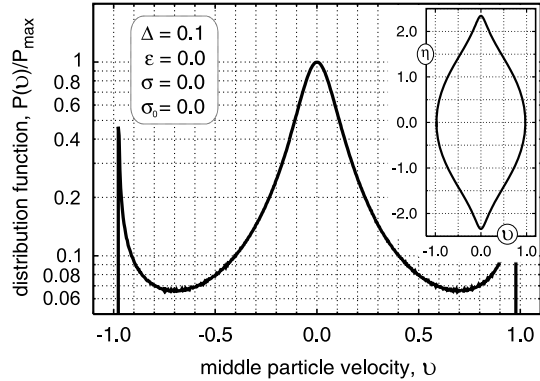


Fig. 3. An example of the velocity distribution $\mathcal{P}(v)$ formed by the movable particle of the 3-particle ensemble without noise and dissipation ($\epsilon = 0$ and $\sigma = 0$). The path on the phase plane $\{\eta, v\}$ formed by this particle is shown in the included window. In numerical simulation $\Delta = 0.1$ was used and a phase path of the velocity amplitude about unity was chosen.

particle system admits conservation of a certain “energy” and the phase paths form a collection of closed curves on the $\{\eta, v\}$ -plane [17].

If the dynamical trap effect is absent, $\Delta = 1$, all these distributions, as it must, are of the Gaussian form shown in Fig. 2 with dotted lines.

3.2 Multi-particle ensemble

To analyze cooperative phenomena arising in such systems the dynamics of 1000-particle ensembles was implemented. Let us, first, consider local properties exhibited by these ensembles. The term “local” means that the corresponding state variable can take practically independent values when the particle index i changes by one or two. The variable η_i (expression (3)) may be regarded in such a manner. It describes the symmetry of particle arrangement in space, when $\eta_i = 0$ particle i takes the middle position between the nearest neighbors, particles $i - 1$ and $i + 1$. A nonzero value of η_i denotes its deviation from this position, in other words, a local distortion of the ensemble symmetry. The latter was the reason for the used name of the variables η_i as well as the variables $v_i = d\eta_i/dt$.

Figure 4 exhibits the found distributions of the variables η and v depending on the dissipation rate σ and the initial distance l between the particles, i.e. their mean density. Comparison of Fig. 2 and Fig. 4 shows us that in this case of weak dissipation the distribution functions of the symmetry distortion $\mathcal{P}(\eta)$ and the distortion rate $\mathcal{P}(v)$ are qualitatively similar to those of the corresponding 3-particle ensemble. Only a few new features appear. First, for the system with high particle density ($l = 5$) a small spike is visible at the center, $\eta = 0$, of the distribution function $\mathcal{P}(\eta)$, which is pronounced in the case of strong dissipation. It corresponds to the symmetrical state of the particle ensemble being stable without dynamical traps and destroyed for the 3-particle ensemble. In the given

case “many-particle” effects seem to reconstruct it in part. So in the given case the particle arrangement is characterized by three states, two of them match the extrema of the distribution function $\mathcal{P}(\eta)$ and the symmetrical state singled out to a some degree.

As for the 3-particle ensemble the distortion rate distribution is again composed of two monoscale components, narrow and wide ones. Previously we have related them to the fast and slow motions. Figure 4 (upper second window) also justifies this. The narrow component is due to the particle motion inside the trap region and should be practically independent of the mean distance between particles. By contrast, the wide one is to depend remarkably on the particle density because it matches the fast motion of particles outside the trap region and, thus, has to be affected by their relative dynamics. Exactly this effect is demonstrated in Fig. 4 visualizing also the corresponding properties of the particle paths.

For the 1000-particle ensemble with strong dissipation, $\sigma \approx 1.0$, the situation changes dramatically, although the characteristic scales of the corresponding distributions turn out to be of the same order in magnitude. In the given case the distribution function $\mathcal{P}(\eta)$ of the symmetry distortion has only one maximum at $\eta = 0$, however, its form is to be characterized by two scales. In other words, it looks like a sum of two monoscale components. One of them is sufficiently wide, its thickness is about the same value that is obtained for the corresponding particle ensemble with weak dissipation. Exactly this component exhibits a remarkable dependence of the particle density, enabling us to relate it to the particle motion outside the trap region. The other is characterized by an extremely narrow and sharp form shown in detail in the inner window in Fig. 4 for the dense particle ensemble. Its sharpness leads us to the assumption that “many-particle” effects in such systems with dynamical traps cause the symmetrical state to be singled out from the other possible states in properties.

By contrast, the distortion rate behaves rather similar to the previous case except for some details. When the mean particle density is high ($l = 5$) the wide component of the distortion rate distribution disappears and only the narrow one remains, with the latter having a quasi-cusp form $\propto \exp\{-|\vartheta|\}$. For the system with low density the peak of the distortion rate distribution splits into two small spikes.

These features can be explained by applying to the low row right windows in Fig. 4, which exhibit typical path fragments formed by motion of a single particle on the $\{\eta, v\}$ -plane. Roughly speaking, now three motion types can be singled out: some stagnation inside a narrow neighborhood of the origin $\{\eta = 0, v = 0\}$ (visible well in the right window), slow wandering inside the trap region that, on the average, follows a line with a finite positive slope (clearly visible in the left window), and the fast motion outside the trap region (visible again in the left window). The fast motion fragments typically stem from an arbitrary point of the low motion region and lead to a certain neighborhood of the origin. It seems that for the system

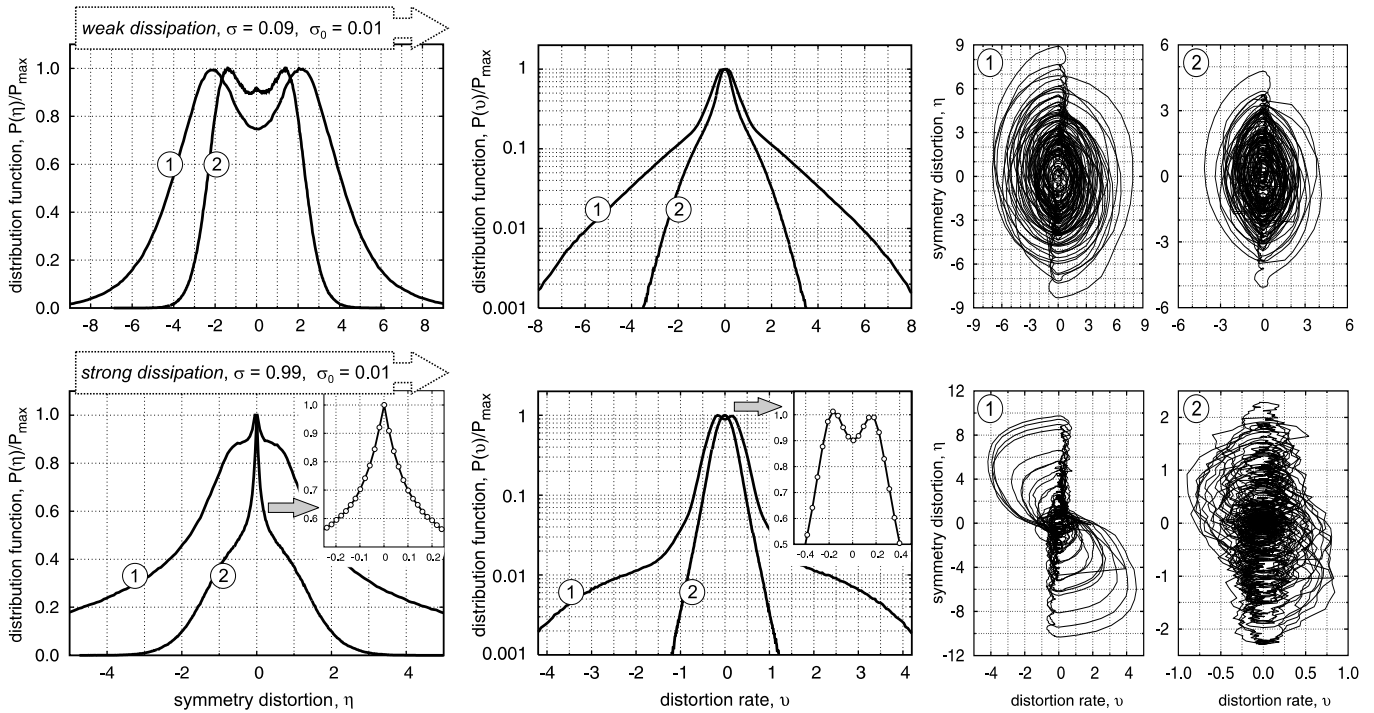


Fig. 4. The distribution functions of the symmetry distortion η and the distortion rate ϑ for the 1000 particle ensemble with low ($l = 50$, label 1) and high ($l = 5$, label 2) density and weak ($\sigma \approx 0.1$) and strong ($\sigma \approx 1.0$) dissipation. The right four windows depict characteristic path fragments of duration of 1000 time units formed by a single particle with index $i = 500$ on the phase plane $\{\eta, \vartheta\}$ which was chosen due to its middle in the given ensemble. The other used parameters are the noise amplitude $\epsilon = 0.1$, the trap effect measure $\Delta = 0.1$, the small regularization friction coefficient $\sigma_0 = 0.01$ and the regularization spatial scale $h_0 = 0.25$. The time interval within which the data were averaged changed from 2000 up to 5000 in order to make the obtained distributions stable.

with low density particles have possibility to go sufficiently far from the origin and during the fast motion come into the stagnation region rarely. As a result, first, the distortion rate distribution function is of a two scale form and contains two spikes on the peak. In the case of high density the fast motion is depressed substantially and the system migrates mainly in the slow motion region entering the stagnation region for many times. So the distortion rate distribution converts into a single-scale function and the appearance of the symmetric state becomes often, giving rise to a significant sharp component of the distortion distribution located near the point $\eta = 0$.

Now we discuss the nonlocal characteristics of the 100-particle ensembles. Figure 5 depicts the velocity distributions. As is seen it depends essentially on both the parameters, the mean particle density and the dissipation rate. When the mean particle density is low and the dissipation is weak ($l = 50$ and $\sigma \approx 0.1$) the velocity distribution is practically of the Gaussian form, however, its width gets extremely large values about 10. We recall that without dynamical traps the width of the corresponding distribution does not exceed 0.5 (Fig. 2). The tenfold increase of the particle density, $l : 50 \mapsto 5$, shrinks the velocity distribution to the same order and its scale gets values similar to that of the distortion rate distribution in magnitude. However in this case the form of the velocity distribution

is a monoscale function of the well pronounced cusp form $\propto \exp\{-|v|\}$. In the case of strong dissipation ($\sigma \approx 1.0$) the situation is opposite. The system with low density ($l = 50$), as previously, is characterized by an extremely wide velocity distribution, its width is about 10. However, now its form deviates substantially from the Gaussian one. For the corresponding ensemble with high density ($l = 5$) the velocity distribution is Gaussian with width about 1. The latter, nevertheless, is much larger than the same width in the absence of dynamical traps.

These features of the velocity distribution characterize the cooperative behavior of particles rather than their individual dynamics. In other words, there should be strong correlations in the motion of not only neighboring particles but also distant ones. Therefore the velocity variations responsible for the formation of such distributions describe in fact the motion of multiparticle clusters. To justify this we apply to the middle column windows in Fig. 5. They visualize some typical fragments of the time patterns formed by the velocities of individual particles. When the mean particle density is low ($l = 50$), these patterns look like a sequence of fragments $\{v_\alpha\}$ inside which the particle velocity varies in the vicinity of some level v_α . The values $\{v_\alpha\}$ are rather randomly distributed inside a certain region of thickness $V \sim 10$ in the vicinity of $v = 0$. The continuous transitions between these fragments occur

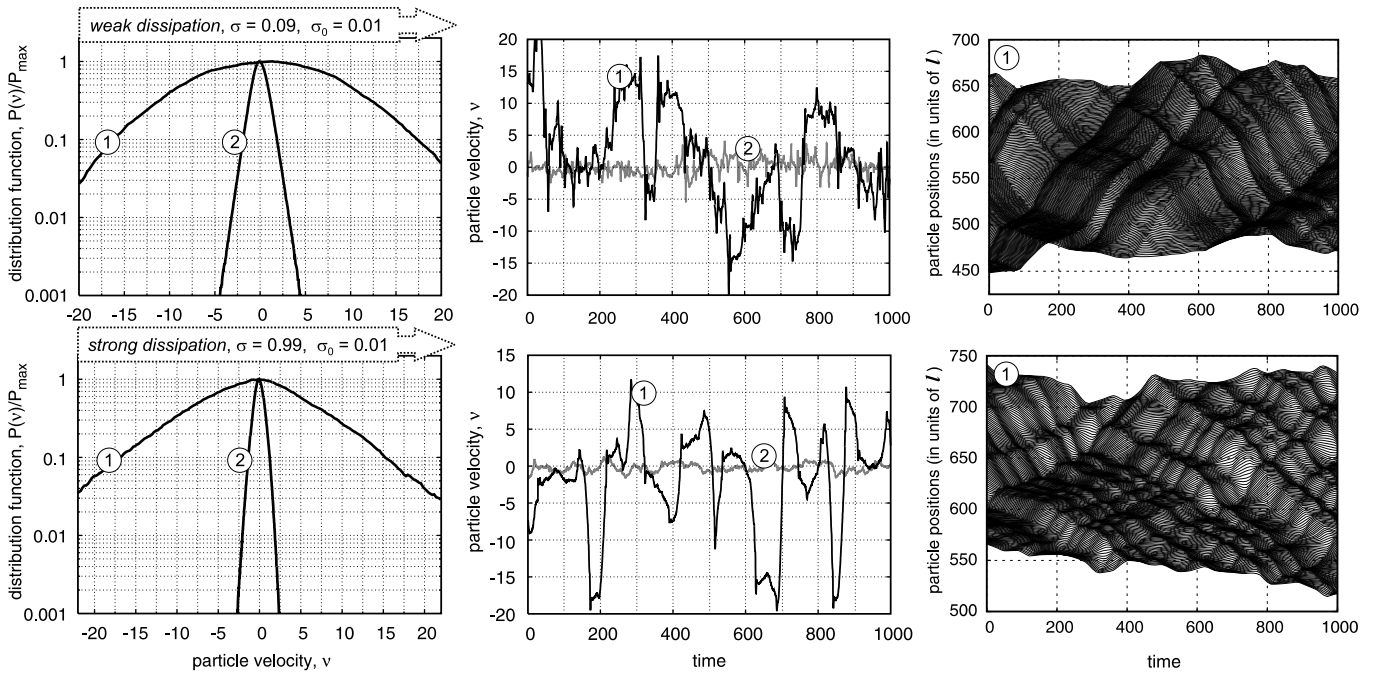


Fig. 5. The distribution functions of the particle velocities and the characteristic time patterns formed by the velocity variations of 500-th particle. Dynamics of the 1000-particle ensemble with low ($l = 50$, label 1) and high ($l = 5$, label 2) mean density and weak ($\sigma \approx 0.1$) and strong ($\sigma \approx 1.0$) dissipation was implemented for the calculation time up to 8000 time units to make the obtained distributions stable with respect to time increase. The right windows visualize the time patterns formed by 200 paths of particle motion during 1000 time units and chosen in the middle of the given ensemble. The other used parameters are the noise amplitude $\epsilon = 0.1$, the trap effect measure $\Delta = 0.1$, the small regularization friction coefficient $\sigma_0 = 0.01$ and the regularization spatial scale $h_0 = 0.25$.

via sharp jumps. The typical duration of these fragments is about $T \sim 100$, which enables us to regard them as long-lived states because the temporal scales of individual particle dynamics are about several units. Moreover, these long-lived states can persist if only a group of many particles moves as a whole because the characteristic distance L individually traveled by a particle involved into such state is about $L \sim VT \sim 1000 \gg l$.

The spatial structure of these cooperative states is visualized in Fig. 5, right column windows. They depict time patterns formed by paths $\{x_i(t)\}$ of 200 particles of duration about 1000 time units. These particles were chosen in the middle part of the 1000-particle ensembles with low density. For high density ensembles such patterns also develop but are not so pronounced. As is seen a large number of different mesoscopic states formed in these systems. They differ from one another in size, the direction of motion, the speed, the life time, *ets.* Moreover, the life time of such a state can be much longer than the characteristic time interval during which particles forming it currently will belong to this state individually. Besides, the found patterns could be classified as hierarchical structures. Some relatively small domains formed by cooperative motion of individual particles in their turn make up together larger superstructures. In other words, the observed long-lived cooperative states have their “own” life independent, in some sense, of the individual particle dy-

namics. The latter properties are the reason for regarding them as certain dynamical phases arising in the systems under consideration due to the dynamical traps affecting the individual particle motion. The term “dynamical” has been used to underline that the complex cooperative motion of particles is responsible for these long-lived states, without the continuous particle motion such states cannot exist.

The obtained results are summarized in the following section.

4 Conclusion

A rather simple model of an oscillator chain, a one-dimensional particle ensemble, with dynamical traps and additive white noise has been considered. It should be noted that the regular “force” governing the individual dynamics of particles has no stationary points except for one matching the system homogeneous state. The latter is locally stable for all the possible values of the system parameters. Nevertheless, as has been demonstrated numerically, the sufficiently strong dynamical trap effect accompanied with white noise gives rise to a wide variety of anomalous and cooperative phenomena.

In particular, the local symmetry of particle arrangement (described by variables (3) called the symmetry distortion) can exhibit kinetic phase transitions. Depending

on the mean particle density and the dissipation rate the distribution function of the symmetry distortion takes either a bimodal form or a twoscale unimodal form, with the latter possessing extremely sharp spike (Fig. 4). The distortion rate distribution also either is characterized by two scales or is of the cusp form $\propto \exp\{-|\vartheta|\}$ smoothed, naturally, inside a narrow transition region.

The cooperative phenomena arising in these system have been studied analyzing the velocity distributions and visualizing some time pattern formed by the particle dynamics. When the mean particle density is sufficiently low the velocity distributions are characterized by the extremely large widths. For the system with high density and low dissipation the velocity distribution function takes also a quasi-cusp form. The visualized time pattern of the velocity dynamics of a single particle has demonstrated the presence of the long-lived states. They look like a sequence of fragments $\{v_\alpha\}$ within which the particle velocity varies in the vicinity of some level v_α continuously joined by sharp jumps in the particle velocity. The velocity levels are rather uniformly distributed inside a wide interval and the life time of these fragments exceeds essentially the time scales of the individual dynamics of particles. It has been shown that such long-lived states can persist if only multiparticle clusters moving as a whole are formed.

The visualized patterns made up of paths of 200 particles have shown also the presence of such cooperative structures. Moreover it has become clear that these long-lived states persist independently in some sense of the individual dynamics of particles forming them currently. In other words, the life time of such a state can exceed substantially the time interval during which the particles forming it at a current time belong to it. Keeping the latter in mind we refer to them as to dynamical states. These states in turn can form superstructures, so the observed patterns are classified as hierarchical structures.

This work was supported in part by DFG Project MA 1508/6, RFBR Grant 02-02-16537, Grant B0056 of Russian Program "Integration", and Moscow Government Grant 1.1.133.

References

1. W. Horsthemke and R. Lefever, *Noise-Induced Transitions* (Springer-Verlag, Berlin, 1984).
2. P. Landa, *Nonlinear Oscillations and Waves in Dynamical Systems*, (Kluwer Academic Publ., Dordrecht, 1996).
3. J. García-Ojalvo and J. M. Sancho, *Noise in Spatially Extended Systems*, Institute for Nonlinear Science (Springer, New York, 1999).
4. V. S. Anishchenko, V. V. Astakhov, A. B. Neiman, T. E. Vadivasova, and L. Schimansky-Geier, *Nonlinear Dynamics of Chaotic and Stochastic Systems*, Springer Series on Synergetics (Springer, Berlin, Heidelberg, and New York, 2002).
5. L. Gammaitoni, P. Hänggi, P. Jung, and F. Marchesoni, *Rev. Mod. Phys.* **70**, 223 (1998).
6. M. Dykman and P. McClintock, *Nature (London)* **391**, 344 (1998).
7. P. Hänggi, P. Talkner, and M. Borkovec, *Rev. Mod. Phys.* **62**, 251 (1990).
8. A. Pikovsky and J. Kurths, *Phys. Rev. Lett.* **78**, 775 (1997).
9. F. Marchesoni, *Phys. Lett. A* **237**, 126 (1998).
10. C. Van den Broeck, J. M. R. Parrondo, and R. Toral, *Phys. Rev. Lett.* **73**, 3395 (1994).
11. C. Van den Broeck, J. M. R. Parrondo, R. Toral, and R. Kawai, *Phys. Rev. E* **55**, 4084 (1997).
12. A. A. Zaikin, L. Schimansky-Geier, *Phys. Rev. E* **58**, 4355 (1998).
13. P. S. Landa, A. A. Zaikin, L. Schimansky-Geier, *Chaos, Solitons, Fractals* **9**, 1367 (1998).
14. A. Zaikin, J. García-Ojalvo, L. Schimansky-Geier, *Phys. Rev. E* **60**, R6275 (1999).
15. P. S. Landa, A. A. Zaikin, V. G. Ushakov, and J. Kurths, *Phys. Rev. E* **61**, 4809 (2000).
16. D. Helbing, *Rev. Mod. Phys.* **73**, 1067 (2001).
17. I. A. Lubashevsky, V. V. Gafiychuk, and A. V. Demchuk, *Physica A* **255**, 406 (1998).
18. I. Lubashevsky, R. Mahnke, P. Wagner, and S. Kalenkov, *Phys. Rev. E* **66**, 016117 (2002).
19. I. Lubashevsky, M. Hajimahmoodzadeh, A. Katsnelson, and P. Wagner, *Eur. Phys. J. B* **36**, 115 (2003).
20. I. Lubashevsky, M. Hajimahmoodzadeh, A. Katsnelson, and P. Wagner *Towards noised-induced phase transitions in system of elements with motivated behavior*, e-print: Arxiv:cond-mat/0310189.
21. A. A. Katsnelson, A. I. Olemskoi, I. V. Suhorukova, G. P. Revkevich, *Physics-Uspekhi* **165**, 331 (1995).
22. P. Wagner and I. Lubashevsky, *Empirical basis for car-following theory development* e-print Arxiv:cond-mat/0311192.
23. K. Burrage and P. M. Burrage, *App. Num. Math.* **22**, (1996) 81.
24. P. M. Burrage, *Numerical methods for stochastic differential equations*, Ph.D. Thesis (University of Queensland, Brisbane, Queensland, Australia, 1999).

